Mapping of shifting tidal estuaries to support Inshore Rescue

Ciara N. McGrath[a], Ruaridh A. Clark[a], Christos Ilioudis[a], Gwilym Gibbons[b], David McKee[cd], Carmine Clemente[a], and Malcolm Macdonald[a]

[a]Department of Electronic and Electrical Engineering, University of Strathclyde, 204 George Street, Glasgow, G1 1XW, United Kingdom.
[b]Creative Help Ltd, Norton House, Wellington Street, Glencaple, Dumfriesshire DG1 4RA, United Kingdom.
[c]Department of Physics, University of Strathclyde, 107 Rottenrow, Glasgow G4 0NG, United Kingdom.
[d]Department of Arctic and Marine Biology, UiT The Arctic University of Norway, Tromsø, Norway

ABSTRACT

Across the world, many coastal tidal regions are unsafe to navigate due to shifting mud and sand pushed by water currents. Ability to regularly map the current location of a channel will aid safe passage for commercial, leisure and rescue craft. This work investigates the use of synthetic aperture radar data derived from satellites to provide accurate mapping of moving channels in coastal regions. As images must be collected at low tide, data availability is assessed considering the relationship between the orbital motion of the satellites and the tides. Change detection methods are applied to suitable images to map changes in the location of navigable channels. Pixels that undergo similar changes over time (e.g. from water covered to exposed sand) are grouped together by examining the principal component of the covariance matrix, for a vector composed of pixel values from the same location at different times. The Solway Firth in Great Britain is selected as a trial site as it is exposed to some of Europe's fastest tidal movements and ranges, and hence is one of Great Britain's most treacherous stretches of coastline.

Keywords: Satellite data, synthetic aperture radar, change detection, tidal estuaries, coastal navigation.

1. INTRODUCTION

Many of the world's estuary channels are uncharted and unsafe to navigate due to shifting mud and sand pushed by water currents. An example of such an uncharted region, the Solway Firth in Great Britain, is shown in Fig. 1.

At present, vessels operating in areas around the world with large tidal ranges and shifting sands rely on local knowledge and hope that channels have not moved since the last known safe passage. As a result, there are areas of prime fishing, leisure and commercial traffic that are under used. For rescue services who need to navigate at speed in the absence of meaningful charts or any visible marine markers at night, knowing the course of the channel is vital to reach casualties, without becoming casualties themselves.

Today, estuaries with shifting channels must be regularly mapped by manually taking depth soundings. As an example, Nith Inshore Rescue take fortnightly trips around the Solway Firth, mapping channels that will be safe for them to use in case of an emergency call out. This is time consuming and labour intensive, and the risk exists that a map may become outdated without their knowledge. The COVID-19 pandemic of 2020 forced Nith Inshore Rescue to reduce the frequency of these mapping trips, further increasing the risk that their navigational charts may be out-of-date. An inaccurate chart could lead to a need to reroute mid-rescue, or in the worst case, to the lifeboat running aground and endangering the rescue team. This is a global issue, which means

Further author information: (Send correspondence to C.N.M.)
C.N.M.: E-mail: ciara.mcgrath@strath.ac.uk

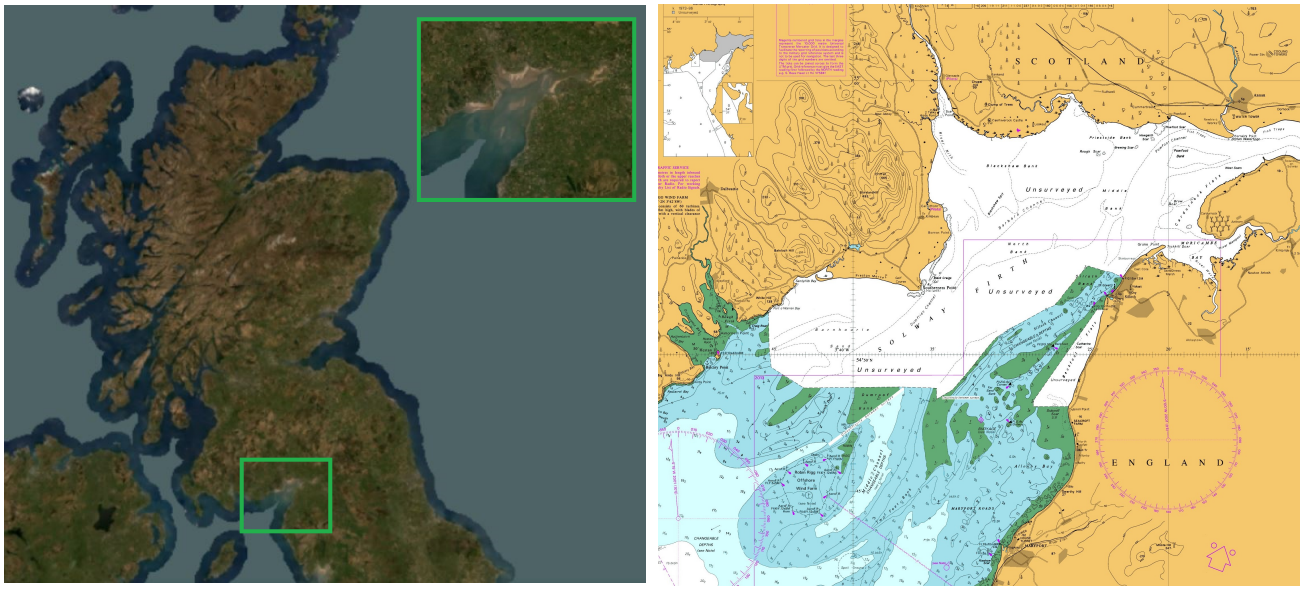

Figure 1: (Left) Location of the Solway Firth, Great Britain.[1] (Right) Navigational chart showing uncharted Solway Firth region.[2] *

that estuaries world-wide remain dangerous, unnavigable and under-utilised. As such, a systematic method of monitoring and mapping the current location of a channel would aid safe passage for commercial, leisure and rescue craft worldwide.

Satellite imagery, which can provide regular, frequent, high-resolution observations of the globe, is an ideal source of information for mapping both land and water features.[3–6] For remote mapping of tidal estuaries, the data must be sufficiently high resolution to identify navigable channels, must be taken at, or around, low tide in order for channels to be visible, and must be updated at least every two weeks, in order to improve upon the current update frequency available through manual charting. Synthetic aperture radar (SAR) imagery is a particularly promising candidate for this, as its ability to penetrate cloud cover provides improved reliability compared to visual imagery.

Change detection is one of the most powerful applications of SAR images. It enables the identification of temporal changes within a given scene starting from a pair of co-registered SAR images representing an area of interest.[7,8] Change detection can be performed by using incoherent or coherent approaches. The former is demonstrated in this paper and attempts to detect changes in the mean power level of a given scene, exploiting only the intensity information from the available images (thus neglecting phase information[9]). The latter jointly analyses both amplitude and phase from the reference and the test data to detect possible changes in the region of interest. Stojanovic and Novak[9] provide a thorough comparison between incoherent and coherent change detection strategies, including the Maximum Likelihood Estimate (MLE) of the SAR coherence parameter, based on high resolution (0.3 m×0.3 m) SAR images. Rignot and Van Zyl[10] present several techniques for change detection and compare these based on their probability of error and on results obtained using repeat-pass ERS-1 SAR data. Recent advances in Coherent Change detection based on polarimetric SAR are presented by Carotenuto et al.[11,12] However, the use of polarimetric information is limited by the reduced availability of polarimetric data as these require higher cost systems to be captured.

This paper investigates the suitability of satellite data that is publicly available through the Copernicus programme[13] to provide up-to-date mapping of tidal estuaries. The Solway Firth, one of the most treacherous bodies of water in Great Britain, is selected as the trial site due to its known propensity for dangerous, shifting

channels. Data availability is assessed considering the spacecraft revisit period and its synchronicity with the local tidal variation. A novel change detection method is presented that performs pixel-wise comparisons to identify and categorise changes in the Solway Firth. This method could form the basis of a channel change alert system for seafarers world-wide.

2. SATELLITE DATA ASSESSMENT

The EU Copernicus Programme freely distributes satellite data, including that collected by the Sentinel-1 and Sentinel-2 spacecraft.[13]

2.1 Data suitability

The Sentinel-2 mission consists of two spacecraft, Sentinel-2 A and Sentinel-2 B, that collect multi-spectral imagery in 13 bands across the visual, near-infra-red (NIR) and short-wave infra-red (SWIR) portions of the spectrum at spatial resolutions ranging from 10m - 60m.[14] This imagery is valuable as the differentiation between water and sand is distinct, particular when using the Normalized Difference Water Index (NDWI). The NDWI is derived from the visible green and the near-infrared bands.[15] For Sentinel-2, these are band B3, which is 560 nm, and band B8, which is 842 nm, respectively. The NDWI is calculated as NDWI= $\frac{B3-B8}{B3+B8}$. An NDWI image of the Solway Firth is seen in Figure 2 where the water is clearly seen in blue. However, visual data cannot be collected at night and cannot penetrate cloud cover, which limits the number of usable images available.

The Sentinel-1 mission also consists of two spacecraft, Sentinel-1 A and Sentinel-1 B. The Sentinel-1 spacecraft collect C-band synthetic aperture radar (SAR) data with a spatial resolution of 5m $\times$ 20m in interferometric wide-swath (IW) mode.[16] This active form of remote sensing can be used at any time of day or night and can image the Earth's surface even through cloud cover. The Sentinel-1 spacecraft are dual polarised, with both transmission and acquisition possible in either horizontal (H) or vertical (V) polarisation. In the vertically transmitted, horizontally received data (VH), the signals returned from the wet sand and water channels appear similar. In the vertically transmitted, vertically received data (VV) however, the distinction between the water and the wet sand is apparent, as seen in Fig. 3.

2.2 Data availability

In order to determine whether sufficient data would be available from the Sentinel-1 and Sentinel-2 missions, individually or in combination, passes of the Solway Firth region are examined for each mission. According to the European Space Agency (ESA) Sentinel User Guides,[17,18] Sentinel-1 will provide approximately daily coverage of Europe, while Sentinel-2 will provide coverage of Europe approximately every two days. Using the Copernicus Open Access Hub,[19] the actual passes of the Sentinel-1 and Sentinel-2 spacecraft over the Solway Firth are determined for for one month from 01/05/2020 - 31/05/2020. Extrapolating based on the repeating

Figure 2: NDWI image of the Solway Firth at low tide processed from Sentinel-2 data. Blue shows location of water channels.

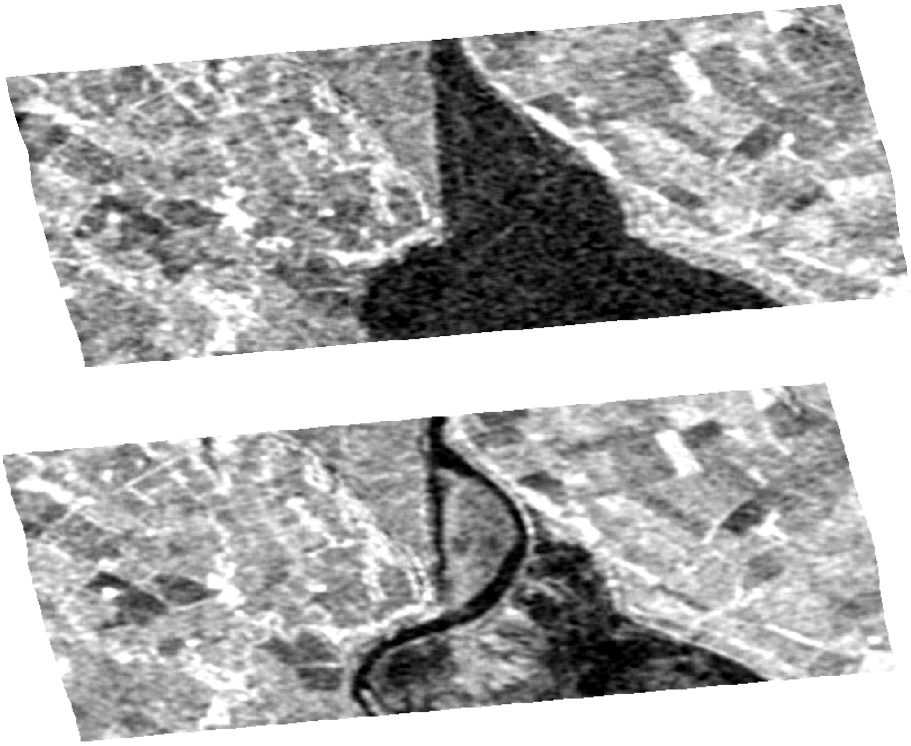

Figure 3: Comparison of images using the VH (above) and VV (below) bands. Images taken of the Solway Firth by Sentinel-1 on June 6th 2020.

cycle of the spacecraft orbits, the data that will be collected of the Solway Firth region is then estimated for a three month period from 01/05/2020 – 31/07/2020. The tidal conditions of the region for the same period are approximated assuming a 12hr 25min period from low tide to low tide, with the first low-tide occurring at 03:48 on 01/05/2020. The actual tidal period of the Solway Firth region will vary; however, this approximation is suitable to estimate the number of usable images that could be collected over an extended time period. Data is assumed to be usable if the spacecraft image acquisition of the region occurs within 3 hours 6 minutes and 15 seconds of the minimum; assuming a symmetrical tidal variation this corresponds to the time period when the tide is $< 50\%$ of maximum.

In the three month period from 01/05/2020 - 31/07/2020, 37 passes of the Solway Firth by Sentinel-2 A and B are identified, of which 18 occur at low tide. The median time between viewings is three days and the maximum time between viewings is 10 days. Assuming a 50% liklihood of cloud cover, this would mean that nine usable images would be available in this three month period.

In the same three month period from 01/05/2020 - 31/07/2020, 77 SAR images from Sentinel-1 A and B are identified, with 36 of these occurring at low tide. As the SAR images are unaffected by cloud, all of these images can be assumed to be usable. 19 of these images cover only a portion of the Firth, while the other 17 cover the full region of interest. The maximum time between usable SAR images is 11 days and the median time between usable SAR images is one day.

From the data availability analysis performed, it can be determined that SAR imagery from Sentinel-1 provides an ideal data source to observe the changing locations of channels in the Solway Firth. Due to the global coverage provided by Sentinel-1 A and B, it can be assumed that the data would be similarly available for tidal estuaries worldwide, with some variation in availability expected depending on the latitude of the region. Visual imagery from Sentinel-2 could provide an additional, complementary data source, but for the purposes of this paper, SAR data from Sentinel-1 will be the primary focus.

3. CHANGE DETECTION METHODOLOGY

3.1 SAR image preparation

SAR data used in this work is obtained from the Sentinel-1 spacecraft via the Copernicus Open Access Hub.[19] This data is then processed using the European Space Agency Sentinel Application Platform (SNAP).[20] The data is radiometrically calibrated to obtain the normalized radar cross section (σ_0)[21] and converted to a decibel scale. A Lee speckle filter[22] with an X and Y filter size of 5 is used. To obtain the final images, a terrain correction using the SRTM Digital Elevation Model[23] and the world geodetic system 1984 map projection[24] is applied. The resulting data are then exported as images for further analysis.

3.2 Image registration

Terrain correction does not guarantee that images of the same location will overlap exactly. Therefore the images are registered by computing the normalised cross-correlation in two-dimensions.[25,26] This is implemented by assessing the correlation coefficient for a range of horizontal and vertical offsets for one of the images.[27] The scaling of this image is also adjusted by first assessing whether increasing or decreasing the scaling increases the maximum correlation coefficient that can be achieved through offsetting. If scaling improves the match, the optimal scaling is sought by adjusting the scaling parameter to maximise the correlation coefficient after offsetting. This cross-correlation can be conducted by comparing the entire first image with the second, but this can produce erroneous results if the river undergoes severe change. Instead, an area exhibiting little change is selected, in this case the surrounding farmland, and used as the basis for determining the optimal scaling and offset to match the two images.

3.3 Detecting and categorising change

Once aligned, images are compared to determine not just that change has occurred but also the type of change. The method, introduced here, determines what change, if any, each pixel has undertaken between the two images, as well as the magnitude of that change. For a comparison of two greyscale SAR images, this change is essentially limited to whether pixels become darker, lighter or remain similar. For the case of shifting sands, this equates to river channels becoming filled with sand (dark pixels becoming lighter) and sand covered areas becoming a channel (light to dark).

The pixel-wise comparison is achieved by assessing the principal component of the covariance matrix, for a vector composed of pixel values from the same location at different times. Once these principal component vectors have been assessed, they are embedded in a Euclidean space and grouped together based on their alignment to one of a number of pixels that undergo the most prominent changes between the two images. This grouping method has been detailed previously for network community detection using a Euclidean space defined by the network's dominant eigenvectors.[28] The pixels that are most prominent are far from the origin of this Euclidean space and have the largest scalar projection in the direction of their position vector when compared with all other pixels. To reduce computation only the top 50,000 pixels, which are furthest from the origin, are considered as potential group leaders. Once these group leaders have been identified, the scalar projection of each pixel with respect to these leaders are assessed to identify the leader and group each pixel is to be assigned to. For the assessment of shifting sands using SAR imagery, this provides a greater division of pixel change than is necessary. Therefore, the groups are split according to the sign of the mean first element of the principal component, which represents the x-axis in the Euclidean space used to define the groups. The two image case is the simplest application of this change detection and categorisation approach, where more images would result in more dimensions of the Euclidean space and grouped pixels would give more complicated insights on the journey a pixel has taken through multiple images.

When presenting the changes detected between the two images, separate colours are used to highlight the two directions of pixel change with the saturation and brightness displayed based on each pixel's distance from the origin of the Euclidean space. Finally, the focus of this paper is on detecting shifting sands, therefore, a threshold is applied so that change is only presented for pixels that either were or became part of the river channel. This threshold was empirically identified as a pixel value of less than 65 in the greyscale SAR images and is applied to the earlier dated image when considering pixels grouped for becoming lighter (new sand), and applied to the later dated image when considering pixels that become darker (new channel).

4. RESULTS

The shifting sand and river channels are displayed in Fig. 4 **a**, in images taken by the Sentinel-1 spacecraft on (from top to bottom) the 26th February 2020, the 25th April 2020 and the 6th June 2020. The detection and categorisation of changes in the river bed are displayed in Fig. 4 **b** and **c**, where new channels and sand banks are clearly highlighted. The comparison between February and April, Fig. 4 **b**, results in the most dramatic change where a large, central, sand bank forms that diverts the river around it. The changes between April and June are subtler but there is a clear narrowing of the channel at the bottom of Fig. 4 **c** that could be cause for concern for anyone looking to navigate these waters. These images are terrain corrected, as detailed in Section 3.1, but adjustments are still required to align the images exactly with overlap of these images presenting as artifacts at the top and bottom edges of Fig. 4 **b**.

It is worth noting that the categorisation of a pixel as "new sand" in Fig. 4 does not necessarily mean that sand is exposed. The "new sand" categorisation simply reflects that a collection of pixels are becoming lighter, which could be due to the channel becoming shallower rather than fully transitioning to sand. Therefore, change is being detected rather than the presence of sand or water. It is, however, likely that in areas of greatest change, denoted by dark colouring in Fig. 4 **b** and **c** that sand or water are present in the latest image.

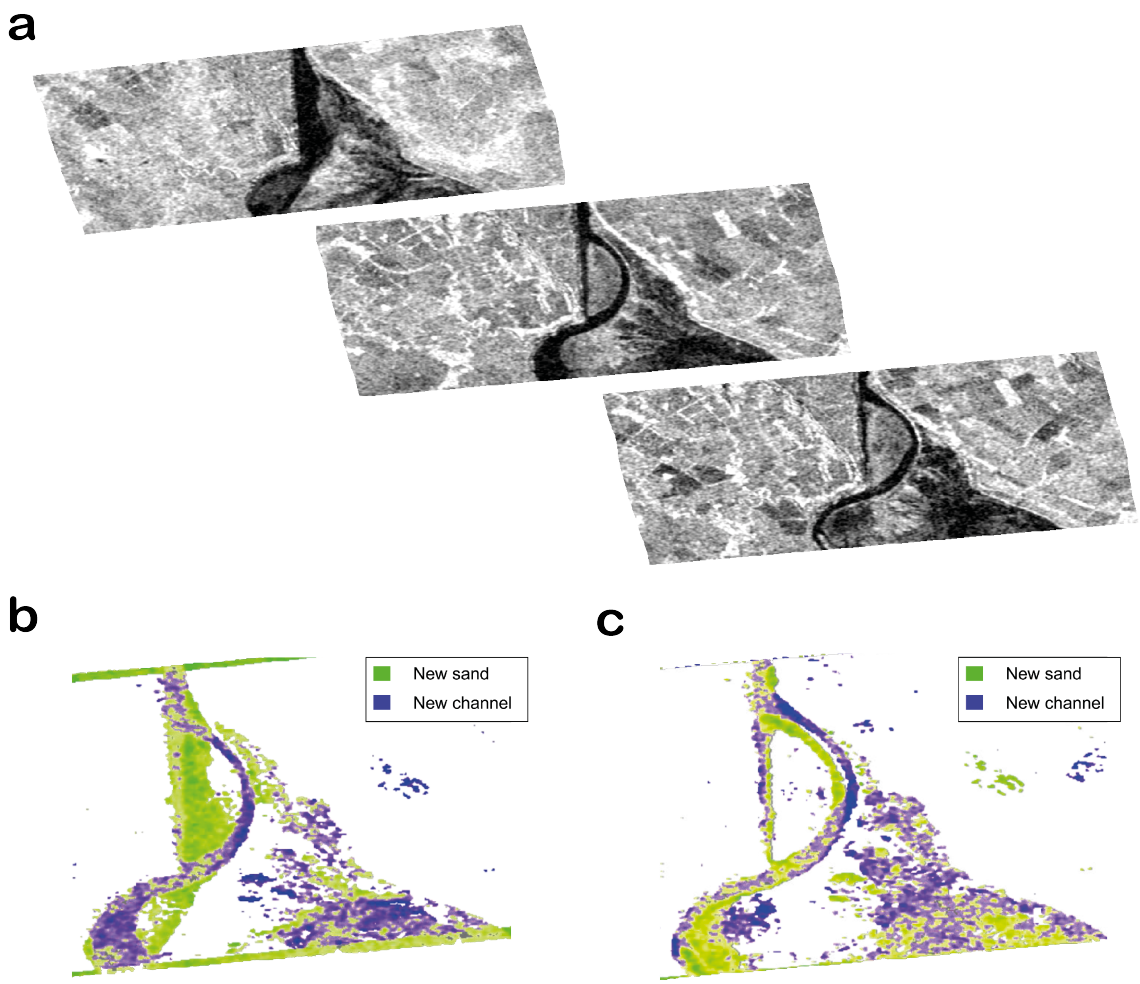

Figure 4: Results of change detection and categorisation on **a** SAR images from February, April and June 2020 (top to bottom), with **b** detailing the emergence of sand or a river channel between February and April, and **c** detailing the changes between April and June.

5. CONCLUSIONS AND FUTURE WORK

The Sentinel-1 and 2 missions pass over the Solway Firth with a median time between viewings of one and three days, respectively; however, the ability of Sentinel-1 synthetic aperture radar to penetrate cloud makes it a more reliable and suitable data source to provide frequent updates on the locations of moving estuary channels. Channel locations can be easily differentiated from surrounding wet sand using the vertically transmitted - vertically received channel of Sentinel-1's synthetic aperture radar instrument. A pixel-wise change detection and categorisation approach that compares pixel intensity from co-registered synthetic aperture radar images can be used to identify changes in river channels. This approach not only detects the presence of significant changes but also provides clarity on how the river channels have shifted through the "new sand" and "new channel" categorisations. This change detection could be enhanced by using the full range of data available from the radar, such as interferometric readings, to provide additional insights.

ACKNOWLEDGMENTS

The authors would like to acknowledge the support of Nith Inshore Rescue and Creative Help Ltd in the development of this work.

REFERENCES

[1] Planet Team, "Planet application program interface: In space for life on earth." San Francisco, CA (2017).

[2] OceanWise, Using: EDINA Marine Digimap Service, "Raster Charts [TIFF geospatial data], Scale 1:50000, Tiles: 1344-0,2013-1,2013-2,2013-3,2013-4,2013-5,2198-1,1320-0,1346-0,2013-0,2093-0,2094-0,2198-0,2199-0,0002-0,1121-0,1411-0,1826-0,2182B-0,2635-0,2724-0,." https://digimap.edina.ac.uk, Downloaded: 2020-08-25 12:34:08.703 (Updated: 16 July 2020).

[3] Mena, J. B. and Malpica, J. A., "An automatic method for road extraction in rural and semi-urban areas starting from high resolution satellite imagery," *Pattern recognition letters* **26**(9), 1201–1220 (2005).

[4] Jin, X. and Davis, C. H., "An integrated system for automatic road mapping from high-resolution multispectral satellite imagery by information fusion," *Information Fusion* **6**(4), 257–273 (2005).

[5] Gupta, A. and Liew, S. C., "The Mekong from satellite imagery: A quick look at a large river," *Geomorphology* **85**(3-4), 259–274 (2007).

[6] Lu, S., Wu, B., Yan, N., and Wang, H., "Water body mapping method with HJ-1A/B satellite imagery," *International Journal of Applied Earth Observation and Geoinformation* **13**(3), 428–434 (2011).

[7] Preiss, M. and Stacy, N., "Coherent change detection: Theoretical description and experimental results," tech. rep.

[8] Touzi, R., Bruniquel, J., and Vachon, P. W., "Coherence estimation for SAR imagery," *IEEE Transactions on Geoscience and Remote Sensing* **37**(1), 135–149 (1999).

[9] Stojanovic, I. and Novak, L., "Change detection experiments using Gotcha public release SAR data," in [*Proc. SPIE 8746, Algorithms for Synthetic Aperture Radar Imagery XX*],

[10] Rignot, E. and Van Zyl, J. J., "Change detection techniques for ERS-1 SAR data," *IEEE Transactions on Geoscience and Remote Sensing* **31**(4), 896–906 (1993).

[11] Carotenuto, V., De Maio, A., Clemente, C., Soraghan, J., and Alfano, G., "Forcing scale invariance in multipolarization SAR change detection," *IEEE Transactions on Geoscience and Remote Sensing* **54**, 36–50 (1 2016).

[12] Carotenuto, V., De Maio, A., Clemente, C., and Soraghan, J., "Invariant rules for multi-polarization SAR change detection," *IEEE Transactions on Geoscience and Remote Sensing* **53**, 3294–3311 (6 2015).

[13] The European Union, "Copernicus: The European Union Earth observation programme," tech. rep. (2019).

[14] Drusch, M., Del Bello, U., Carlier, S., Colin, O., Fernandez, V., Gascon, F., Hoersch, B., Isola, C., Laberinti, P., Martimort, P., et al., "Sentinel-2: ESA's optical high-resolution mission for GMES operational services," *Remote Sensing of Environment* **120**, 25–36 (2012).

[15] McFeeters, S. K., "The use of the normalized difference water index (NDWI) in the delineation of open water features," *International Journal of Remote Sensing* **17**(7), 1425–1432 (1996).

[16] Geudtner, D., Torres, R., Snoeij, P., Davidson, M., and Rommen, B., "Sentinel-1 system capabilities and applications," in [*2014 IEEE Geoscience and Remote Sensing Symposium*], 1457–1460, IEEE (2014).

[17] European Space Agency, "Sentinel-1 observation scenario." Available at https://sentinel.esa.int/web/sentinel/missions/sentinel-1/observation-scenario. Accessed: 20/08/2020).

[18] European Space Agency, "Sentinel-2 revisit and coverage." Available at https://sentinel.esa.int/web/sentinel/user-guides/sentinel-2-msi/revisit-coverage. Accessed: 20/08/2020).

[19] European Space Agency, *Copernicus Open Access Hub 2020* (accessed August 10, 2020). https://scihub.copernicus.eu/.

[20] European Space Agency, *Sentinel Application Platform (SNAP)* (accessed August 21, 2020). https://step.esa.int/main/toolboxes/snap/.

[21] Miranda, N. and Meadows, P., "Radiometric calibration of S-1 Level-1 products generated by the S-1 IPF," tech. rep. (2015).

[22] Lee, J.-S., "Speckle suppression and analysis for synthetic aperture radar images," *Optical Engineering* **25**(5), 636 – 643 (1986).

[23] Rabus, B., Eineder, M., Roth, A., and Bamler, R., "The shuttle radar topography mission—a new class of digital elevation models acquired by spaceborne radar," *ISPRS Journal of Photogrammetry and Remote Sensing* **57**(4), 241–262 (2003).

[24] Decker, B. L., "World geodetic system 1984," tech. rep., Defense Mapping Agency Aerospace Center (1986).

[25] Lewis, J., "Fast normalized cross-correlation, 1995," in [*Vision Interface*], **2010**, 120–123 (2010).

[26] Pallotta, L., Giunta, G., and Clemente, C., "Subpixel SAR image registration through parabolic interpolation of the 2D cross-correlation," *IEEE Transactions on Geoscience and Remote Sensing* **58**, 4132–4144 (6 2020).

[27] MathWorks, "normxcorr2: Normalized 2-D cross-correlation." https://uk.mathworks.com/help/images/ref/normxcorr2.html (2020).

[28] Clark, R., Punzo, G., and Macdonald, M., "Network communities of dynamical influence," *Scientific Reports* **9**(1), 1–13 (2019).